New measurement of the g factor of the $^{54}Cr(2_1^+)$ state and its shell model interpretation

S. Wagner,[1] K.-H. Speidel,[1] O. Kenn,[1] R. Ernst,[1] S. Schielke,[1] J. Gerber,[2] P. Maier-Komor,[3] N. Benczer-Koller,[4] G. Kumbartzki,[4] Y.Y. Sharon,[4] and F. Nowacki[5]

[1]*Institut für Strahlen-und Kernphysik, Universität Bonn, Nußallee 14-16, D-53115 Bonn, Germany*

[2]*Institut de Recherches Subatomique, F-67037 Strasbourg, France*

[3]*Physik-Department, Technische Universität München, James-Franck-Strasse, D-85748 Garching, Germany*

[4]*Department of Physics and Astronomy, Rutgers University, New Brunswick, New Jersey 08903*

[5]*Laboratoire de Physique Théorique, 3-5 rue de l'Université, F-67084 Strasbourg Cedex, France*

(Received 11 May 2001; published 22 August 2001)

The g factor of the first 2^+ state of ^{54}Cr was remeasured employing the combined technique of projectile Coulomb excitation in inverse kinematics and transient magnetic fields. The value obtained, $g=+0.840(56)$, is significantly larger than previous data. The new value agrees better with a truncated than with a large-scale shell model calculation. The present result is discussed in the context of recently determined g factors of the first 2^+ states of ^{50}Cr and ^{52}Cr as well as $B(E2)$ values determined from lifetime measurements.

DOI: 10.1103/PhysRevC.64.034320 PACS number(s): 21.10.Ky, 25.70.De, 27.50.+e

I. INTRODUCTION

Recent measurements of magnetic moments and lifetimes of the first 2^+ and 4^+ states of Ti and Cr nuclei have yielded new insights into the single-particle structure of fp shell nuclei [1–3]. This progress was made possible by a higher experimental precision and new large-scale shell model (LSSM) calculations, in particular, by the assumption of a closed ^{40}Ca core with excitation of both protons and neutrons from the $0f_{7/2}$ shell into the remaining fp shell orbits ($1p_{3/2}$,$0f_{5/2}$ and $1p_{1/2}$). For the first time, both the quality of the calculations in terms of the diagonalization of particle configurations in a large model space and the effect of different effective nucleon-nucleon interactions could be tested by the precise experimental g factors and $B(E2)$ values.

The improvement in the measurements stems from Coulomb excitation of heavy beams by light target nuclei. The γ rays emitted from the excited projectiles were detected in coincidence with recoiling target ions focused forward in the beam direction. This inverse kinematic approach has the additional advantage of producing projectile ions with high velocities. The transient field strength generally increases with ion velocity. The accuracy of g factor determinations is practically limited only by the precise knowledge of the transient field strength under the given experimental conditions. Two empirical parametrizations, the linear parametrization [4] and the Rutgers parametrization [5], have been generally used. However, the most reliable calibration of the transient field is usually obtained through a measurement of a known g factor in a neighboring nucleus under similar kinematic conditions and, if possible, the same target.

The g factors of the 2_1^+ and 4_1^+ states in ^{50}Cr and of the 2_1^+ state of ^{52}Cr have been measured previously with Coulomb excitation [6–8], with a fusion evaporation reaction under different experimental conditions [9] and, more recently, by Coulomb excitation in inverse kinematics [1,2]. The new ^{50}Cr data agree with cranked Hartree-Fock-Bogoliubov [10] and shell model calculations [10,11], which predict $g(4^+)/g(2^+)>1$; in addition, the value of $g(2^+)$ for ^{52}Cr is also in good agreement with the same shell model calculations [3] although it is smaller than that of a previous measurement [8].

The g factor of the first 2^+ state of ^{54}Cr had not been previously measured with comparable accuracy. Two g factor measurements had been reported with statistical uncertainties of about 20%, $g=+0.56(10)$ [6] and $g=+0.53(12)$ [7]. These data do not agree with either the shell model prediction $g=+0.73$ [6,12], or with calculations within the projected Hartree-Fock formalism using band-mixed wave functions, $g=+0.74$ [13].

In a new set of experiments the first 2^+ state of ^{54}Cr was measured under essentially the same experimental conditions as the former Cr experiments [1,2]. The target was prepared under identical conditions and independently checked in measurements of the g factor of the 2^+ state in ^{56}Fe and ^{50}Cr, thus providing a calibration of the transient magnetic field. Hence, the determination of the g factor of the 2_1^+ state of ^{54}Cr relative to the g factor of the lighter Cr isotopes is relatively free from systematic uncertainties pertaining to target and transient field conditions.

The 2_1^+ state of ^{54}Cr was also populated in an α-transfer reaction ^{12}C(^{50}Ti,2α)^{54}Cr. The same target was bombarded by a ^{50}Ti beam. This reaction populates predominantly the first 2^+ state of ^{54}Cr, whereas higher-lying states are only weakly excited. The selectivity of this particular reaction has a character distinctly different from that of a fusion evaporation reaction in which high-energy states are populated and the low-lying states are fed via cascade transitions. The absence of strong feeding in the current experiment ensures a clean measurement of the precession of the magnetic moment of the 2^+ state. The same strength of the α transfer has been observed with other beams of Ti and Cr isotopes [2] as well as with Ni beams [15]. In particular, using a ^{58}Ni beam the g factor of the first 2^+ state of unstable ^{62}Zn was recently measured for the first time [16].

II. EXPERIMENTAL DETAILS

In the present experiments an isotopically pure ^{54}Cr ion beam was provided from natural Cr by the ion source of the

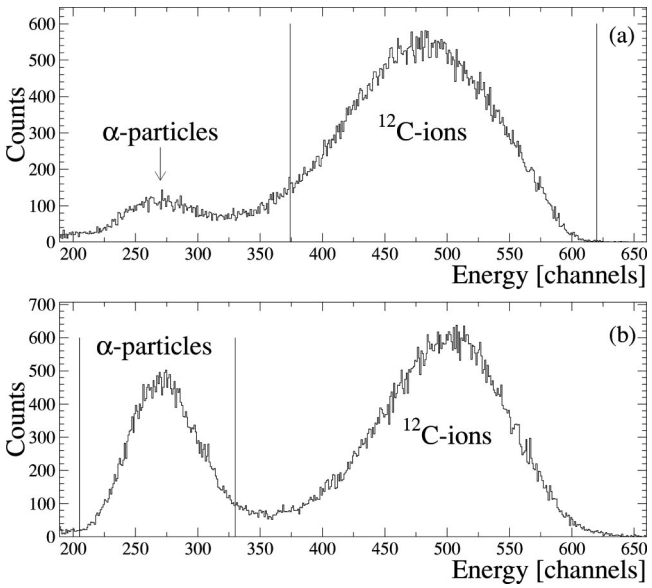

FIG. 1. Particle spectra in coincidence with all γ rays at low bias of the 100 μm Si detector. The α particles are well separated from carbon ions due to incomplete stopping. (a) refers to a 115 MeV ^{54}Cr beam and (b) to a 110 MeV ^{50}Ti beam.

Cologne Tandem accelerator and accelerated to an energy of 115 MeV with intensities of about 1 nA on the target. The beam ions were Coulomb excited to the first 2^+ state by a natural carbon layer on the multilayered target, which consisted of a 0.45 mg/cm^2 ^{nat}C layer deposited on a 3.82 mg/cm^2 gadolinium layer evaporated at 800 K on a 1 mg/cm^2 tantalum foil followed by a 3.5 mg/cm^2 copper layer [14]. The copper backing served as an interaction-free environment stopper for the recoiling Cr ions and provided good thermal conductivity. The target was cooled to liquid nitrogen temperature and magnetized by an external field of 0.06 T.

The γ rays emitted from the excited 2^+ state at 0.835 MeV were measured in coincidence with the forward scattered carbon ions using 12.7 cm$\times$12.7 cm NaI(Tl) scintillators. In addition, an *n*-type, coaxial Ge detector with relative efficiency of 40% was placed at 0° to the beam direction to serve as a monitor for contaminant lines in the energy region of interest. Charged particles, such as carbon ions and α particles from the above-mentioned reactions, were detected in a 100 μm Si counter placed at 0° and subtending an angle of $\pm$15°. The effective detector bias was maintained abnormally low at $\simeq$5 V in order to separate the carbon ions from light charged particles such as protons and α particles, which do not completely stop in the thus reduced depletion layer of the Si detector. The separation of the particle groups is clearly seen in the particle spectra taken in coincidence with all γ rays using a ^{54}Cr or a ^{50}Ti beam (Fig. 1). The low-energy peaks are associated with α particles from the decay of ^{8}Be of the transfer reaction corresponding to ^{58}Fe and ^{54}Cr, respectively. The γ-ray transitions in these nuclei are seen in the coincidence spectra of the Ge detector (Fig. 2). Typical spectra of the NaI(Tl) scintillators obtained in coincidence with the C ions are shown in Fig. 3.

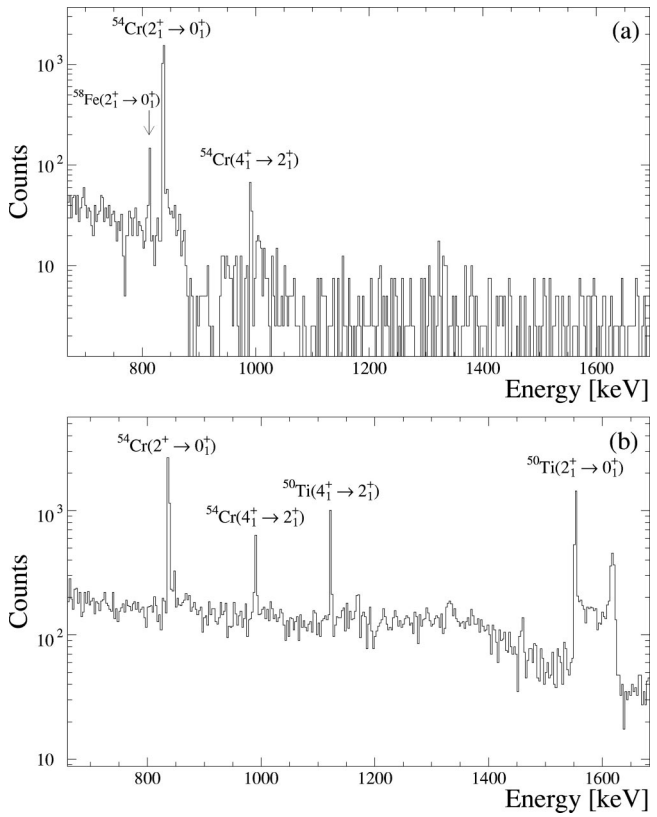

FIG. 2. Ge γ spectra in coincidence with α particles and carbon ions. (a) refers to ^{54}Cr beam and (b) to ^{50}Ti beam. Prominent γ-ray lines result from Coulomb excitation and α-transfer reactions.

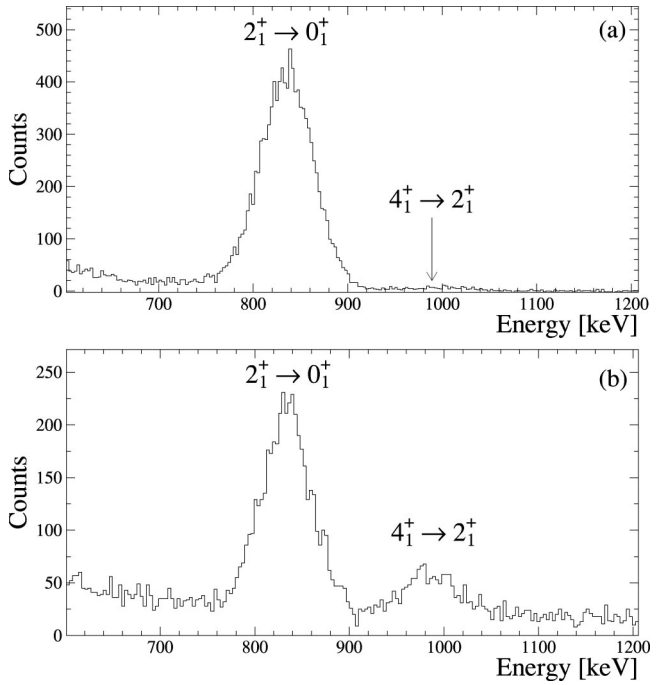

FIG. 3. NaI(Tl) γ spectra of excited ^{54}Cr nuclei in coincidence with (a) carbon ions from collisions with a ^{54}Cr beam and (b) α particles associated with the α transfer to ^{50}Ti beam ions. The $(2_1^+ \to 0_1^+)$ and $(4_1^+ \to 2_1^+)$ γ lines are well resolved.

TABLE I. Summary of the average velocities of the excited ^{54}Cr ions, from reactions with ^{54}Cr and ^{50}Ti beams, entering and exiting the gadolinium foil, the measured logarithmic slopes S of the angular correlations at $|\theta_\gamma| = 65°$. The g factors were derived from the experimental precession angles $\Phi^{\rm expt}$ and calculated $\Phi^{\rm lin}/g$ values using Eqs. (2.1), (3.1), and (3.2). The g factor result of ^{50}Cr(2_1^+) was obtained bombarding the same target with a ^{50}Cr beam.

Nucl. (I^π)	Beam	$E_{\rm beam}$ (MeV)	$\langle v/v_0\rangle_{\rm in}$	$\langle v/v_0\rangle_{\rm out}$	$\lvert S(65°)\rvert$	$\Phi^{\rm expt}$ (mrad)	$\Phi^{\rm lin}/g$ (mrad)	$g(2_1^+)$
^{54}Cr(2^+)	^{54}Cr	115	5.4	2.2	2.486(67)	29.8(27)	34.9(17)	+0.854(88)
		115	5.4	2.2	2.490(55)	29.0(16)	34.9(17)	+0.831(61)
	^{50}Ti	110	6.4	3.2	0.411(62)	45(16)	35.1(17)	+1.28(46)
^{50}Cr(2^+)	^{50}Cr	120	5.7	2.3	2.232(28)	21.58(38)	35.1(17)	+0.615(32) [a]

[a] In good agreement with $g = 0.619(31)$ obtained in Ref. [2].

Particle-γ angular correlations $W(\theta_\gamma)$ and anisotropies $W(\theta_\gamma = 50°)/W(\theta_\gamma = 80°)$ have been measured for both reactions (Coulomb excitation and α transfer) to populate the ^{54}Cr(2^+) state. For the Coulomb excitation reaction where the spin alignment is generally rather large, a measurement of the anisotropy is sufficient to determine the logarithmic slope $S = [1/W(\theta_\gamma)][dW(\theta_\gamma)/d\theta_\gamma]$ in the rest frame of the γ-emitting nuclei at angles $\theta_\gamma = 65°$, where the experimental sensitivity to the spin precessions is optimal. This procedure is described in more detail in Ref. [2]. A complete angular correlation has been measured for the transfer reaction where the alignment was found to be reduced from that observed in the Coulomb excitation reaction in order to determine the corresponding slope value (Table I).

Precession angles $\Phi^{\rm expt}$ were determined as described in former publications [2]. The observed quantities are combined double ratios (DR) of counting rates of coincident γ rays (integrating photopeak intensities only) of detector pairs symmetric to the beam direction with the external magnetizing field perpendicular to the γ-detection plane, alternately in the ''up'' and ''down'' directions. The precession angles are given by [2]

$$\Phi^{\rm expt} = \frac{1}{S}\frac{\sqrt{\rm DR}-1}{\sqrt{\rm DR}+1} = g\frac{\mu_N}{\hbar}\int_{t_{\rm in}}^{t_{\rm out}} B_{\rm TF}(v_{ion}(t))e^{-t/\tau}dt, \tag{2.1}$$

where g is the g factor of the 2^+ state and $B_{\rm TF}$ the transient field acting for the time interval $(t_{\rm out} - t_{\rm in})$ that the ions spend in the gadolinium layer; the exponential accounts for the decay of the excited state with lifetime τ.

III. RESULTS AND DISCUSSION

The g factor of the 2^+ state was derived from the experimental precession angles, $\Phi^{\rm expt}$, by determining the effective transient field strength $B_{\rm TF}$ on the basis of the linear parametrization [4] and given ion conditions:

$$B_{\rm TF}(v_{\rm ion}) = G_{\rm beam}\cdot B_{\rm lin} \tag{3.1}$$

with

$$B_{\rm lin} = a({\rm Gd})\cdot Z_{\rm ion}\cdot\frac{v_{\rm ion}}{v_0}, \tag{3.2}$$

where the strength parameter $a({\rm Gd}) = 17(1)$ T [2], $v_0 = e^2/\hbar$, and $G_{\rm beam} = 0.83(4)$ is the attenuation that accounts for the dynamic demagnetizations induced by the ion beam [17,18]. The value for $G_{\rm beam}$ was taken to be the same as that used for the other Cr isotopes [2] since the beam and target conditions were similar insofar as the relevant parameters such as the stopping power in gadolinium and the occupancy

TABLE II. Comparison of the measured g factors of 2_1^+ states, lifetimes, and $B(E2)$ values, and results from large-scale shell model calculations (LSSM). W.u. denotes Weisskopf units.

Nucl. (I^π)	E_x (MeV)	τ (ps)	$B(E2)$ (W.u.) Expt.	$B(E2)$ (W.u.) LSSM	$g(2_1^+)$ Expt.	$g(2_1^+)$ LSSM
^{50}Cr(2_1^+)	0.783	13.2(4) [a]	19.2(6) [a]	18.3 [a]	+0.619(31) [a]	+0.568 [a]
^{52}Cr(2_1^+)	1.434	1.13(3) [a]	10.3(3) [a]	12.4 [a]	+1.206(64) [a]	+1.172 [a]
^{54}Cr(2_1^+)	0.835	11.4(4) [b]	14.5(6) [b]	15.0	+0.840(56) [c]	+0.625

[a] Reference [2].
[b] Reference [24].
[c] Weighted mean of g (Table I).

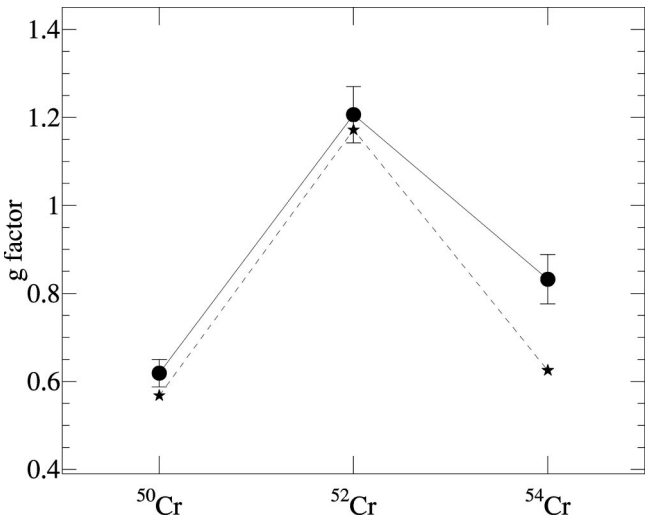

FIG. 4. Comparison of experimental g factors (solid points) of the 2_1^+ states of ^{50,52,54}Cr with large-scale shell model calculations (stars). Lines are drawn to guide the eye.

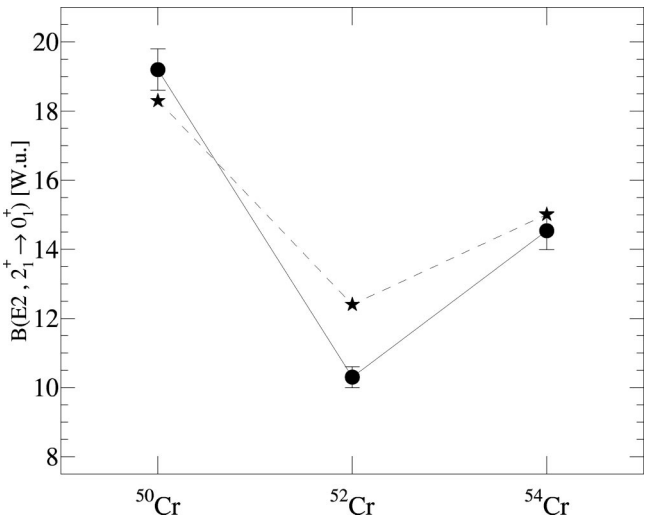

FIG. 5. Experimental $B(E2)$ values of $(2_1^+ \rightarrow 0_1^+)$ transitions of ^{50,52,54}Cr in Weisskopf units (solid points) are compared with results from large-scale shell model calculations (stars). Lines are drawn to guide the eye.

of the electron orbitals of the ions at the given velocity were similar. The precessions $\Phi^{\mathrm{lin}}/\mathrm{g}$ were calculated using Eqs. (2.1), (3.1), and (3.2).

The g factors determined in different experiments are summarized in Table I. The excellent reproducibility of the measurements is demonstrated in the two results from independent runs at 115 MeV. The lower accuracy obtained in the α-transfer reaction has its origin in the small slope of the angular correlation. In addition, the calibration data for the ^{50}Cr measurement taken with the same target are included. The weighted mean average

$$g(^{54}\mathrm{Cr}; 2_1^+) = +0.840(56)$$

of ^{54}Cr is shown in Table II together with the recent g factors of the first 2^+ states of ^{50}Cr and ^{52}Cr [2]. These results have been plotted in Fig. 4. The pronounced peak at ^{52}Cr clearly reflects neutron shell closure at $N=28$ associated with a dominant $(f_{7/2})^4$ proton configuration in the wave function with its Schmidt value $g(\pi f_{7/2}) = +1.655$ (assuming bare values of $g_l = 1$ and $g_s = 5.586$). The lower values of neighboring ^{50}Cr and ^{54}Cr imply significant contributions from two neutron holes in the $f_{7/2}$ shell and two neutrons in the $p_{3/2}$ orbit, respectively. The Schmidt values of these configurations are both negative: $g(\nu f_{7/2}) = -0.547$ and $g(\nu p_{3/2}) = -1.275$.

In order to obtain a better understanding of the effects of well-defined particle configurations on the magnitude of the g factor calculations were carried out with the computer code OXBASH [19] using the FPD6 interaction [20]. The results are summarized in Table III.

The first three rows in the table reflect qualitatively the relative single-particle Schmidt values for a neutron in fp orbitals beyond the $0f_{7/2}$ orbital: $g(\nu p_{3/2}) = -1.275$, $g(\nu p_{1/2}) = +1.275$, and $g(\nu f_{5/2}) = +0.547$. Thus the configuration with $(0f_{7/2})^{12}(1p_{3/2})^2$ has a barely positive g factor, recalling that $g(\pi f_{7/2}) = +1.655$.

In the fourth row of the table, the two nucleons outside the $0f_{7/2}$ orbital were free to be anywhere in the $1p_{3/2}, 1p_{1/2}, 0f_{5/2}$ space. The large occupancy of the $0f_{5/2}$ orbital can be related to its having the same orbital angular momentum as the dominant $0f_{7/2}$ orbital. The small occupancy of the $p_{1/2}$ may reflect the fact that in the $(0f_{7/2})^{12}(1p_{1/2})^2$ configuration, the $(0f_{7/2})^{12}$ cannot be coupled to an angular momentum 0 to obtain a 2^+ state.

The final calculation in the fifth row has either 11 or 12 nucleons in the $0f_{7/2}$ orbital and 3 or 2 in the $(1p_{3/2}, 1p_{1/2}, 0f_{5/2})$ space and yields a g factor $g(2_1^+) = +0.725$. This value, fortuitously, is very close to the value $g(2_1^+) = +0.734$, obtained by Nakada *et al.* [12], with the Kuo-Brown G-matrix interaction in a restricted model space

TABLE III. Comparison of g factor calculations for ^{54}Cr(2^+) with different configuration spaces.

Configuration	Occupancy	$g(2_1^+)$
$(0f_{7/2})^{12}(1p_{3/2})^2$	(12)(2)	+0.0631
$(0f_{7/2})^{12}(1p_{1/2})^2$	(12)(2)	+1.655
$(0f_{7/2})^{12}(0f_{5/2})^2$	(12)(2)	+1.234
$(0f_{7/2})^{12}(1p_{3/2}, 1p_{1/2}, 0f_{5/2})^2$	(12)(0.63, 0.16, 1.21)	+1.044
$(0f_{7/2})^{11-12}(1p_{3/2}, 1p_{1/2}, 0f_{5/2})^{3-2}$	(11.73) (0.76, 0.27, 1.24)	+0.725

in which up to two $f_{7/2}$ particles were excited into higher fp orbits.

For a more quantitative description of the g factor of ^{54}Cr(2_1^+) large-scale shell model (LSSM) calculations were carried out. These calculations include *all* $f_{7/2}$ particles (protons and neutrons) outside the ^{40}Ca core and the whole fp shell configuration space. This large computation was performed with the computer code ANTOINE [21] using the modified version of the Kuo-Brown effective interaction KB3 [22,23]. The same procedure was applied earlier for calculating g factors and $B(E2)$ values of the other Cr isotopes ^{50,52}Cr [2]. As shown in Fig. 4 and Table II, the overall agreement with the LSSM calculation is good. The g factor calculation underestimates the experimental value only for ^{54}Cr. A better agreement was obtained with calculations in a truncated configuration space [12]. The same behavior was found before in the data of the $N=28$ isotones [3] and is still not understood. Possibly the fractionation of the wave function into many components as more $0f1p$ shell excitations are permitted is one of the reasons why the calculated g factor in larger configuration spaces is smaller.

The LSSM calculations, with effective charges of $1.5e$ for protons and $0.5e$ for neutrons [23], also yield good results for $B(E2)$ values as shown in Fig. 5. Evidently, the minimum in the $B(E2)$ of ^{52}Cr relative to the $B(E2)$ values of its neutron-deficient and neutron-rich neighbors reflects the reduced collectivity expected for a semimagic nucleus. Summarizing the present work, the new technique of projectile Coulomb excitation in combination with transient magnetic fields yields g factors of sufficiently high precision to test large-scale shell model calculations and their limits.

ACKNOWLEDGMENTS

The authors are grateful to the operators of the tandem accelerator for their cooperation during the experiments. Support by the BMBF, the Deutsche Forschungsgemeinschaft, and the U.S. National Science Foundation is acknowledged.

[1] R. Ernst, K.-H. Speidel, O. Kenn, U. Nachum, J. Gerber, P. Maier-Komor, N. Benczer-Koller, G. Jakob, G. Kumbartzki, L. Zamick, and F. Nowacki, Phys. Rev. Lett. **84**, 416 (2000).
[2] R. Ernst, K.-H. Speidel, O. Kenn, A. Gohla, U. Nachum, J. Gerber, P. Maier-Komor, N. Benczer-Koller, G. Kumbartzki, G. Jakob, L. Zamick, and F. Nowacki, Phys. Rev. C **62**, 024305 (2000).
[3] K.-H. Speidel, R. Ernst, O. Kenn, J. Gerber, P. Maier-Komor, N. Benczer-Koller, G. Kumbartzki, L. Zamick, M. S. Fayache, and Y. Y. Sharon, Phys. Rev. C **62**, 031301(R) (2000).
[4] J. L. Eberhardt, R. E. Horstman, P. C. Zalm, H. A. Doubt, and G. van Middelkoop, Hyperfine Interact. **3**, 195 (1977).
[5] N. K. B. Shu, D. Melnik, J. M. Brennan, W. Semmler, and N. Benczer-Koller, Phys. Rev. C **21**, 1828 (1980).
[6] C. Fahlander, K. Johansson, E. Karlsson, and G. Possnert, Nucl. Phys. **A291**, 241 (1977).
[7] A. Pakou, R. Tanczyn, D. Turner, W. Jan, G. Kumbartzki, N. Benczer-Koller, Xiao-Li Li, Huan Liu, and L. Zamick, Phys. Rev. C **36**, 2088 (1987).
[8] A. E. Stuchbery, C. E. Doran, A. P. Byrne, H. H. Bolotin, and G. D. Dracoulis, Hyperfine Interact. **36**, 75 (1987).
[9] A. A. Pakou, J. Billowes, A. W. Mountford, and D. D. Warner, Phys. Rev. C **50**, 2608 (1994).
[10] G. Martinez-Pinedo, A. Poves, L. M. Robledo, E. Caurier, F. Nowacki, J. Retamosa, and A. Zuker, Phys. Rev. C **54**, R2150 (1996).
[11] L. Zamick and D. C. Zheng, Phys. Rev. C **54**, 956 (1996).
[12] H. Nakada, T. Sebe, and T. Otsuka, Nucl. Phys. **A571**, 467 (1994).
[13] S. Saini and M. R. Gunye, Phys. Rev. C **24**, 1694 (1981).
[14] P. Maier-Komor, K.-H. Speidel, and A. Stolarz, Nucl. Instrum. Methods Phys. Res. A **334**, 191 (1993).
[15] O. Kenn, K.-H. Speidel, R. Ernst, J. Gerber, P. Maier-Komor, and F. Nowacki, Phys. Rev. C **63**, 064306 (2001).
[16] O. Kenn, K.-H. Speidel, R. Ernst, S. Schielke, S. Wagner, J. Gerber, P. Maier-Komor, N. Benczer-Koller, G. Kumbartzki, and F. Nowacki (unpublished).
[17] K.-H. Speidel, U. Reuter, J. Cub, W. Karle, F. Passek, H. Busch, S. Kremeyer, and J. Gerber, Z. Phys. D **22**, 371 (1991).
[18] G. Jakob, J. Cub, K.-H. Speidel, S. Kremeyer, H. Busch, U. Grabowy, A. Gohla, O. Jessensky, and J. Gerber, Z. Phys. D **32**, 7 (1994), and references therein.
[19] A. Etchegoyen, W. D. Rae, N. S. Godwin, W. A. Richter, C. H. Zimmerman, B. A. Brown, W. E. Ormand, and J. S. Winfield, computer code OXBASH, MSU-NSCL Report No. 524, 1985 (unpublished).
[20] W. A. Richter, M. G. Van der Merwe, R. E. Julies, and B. A. Brown, Nucl. Phys. **A253**, 325 (1991).
[21] E. Caurier, computer code ANTOINE, Strasbourg, 1989.
[22] A. Poves and A. Zuker, Phys. Rep. **70**, 235 (1981).
[23] A. Poves, J. Sanchez-Solano, E. Caurier, and F. Nowacki Nucl. Phys. A (to be published).
[24] H. Junde, S. Huibin, Z. Weizhong, and Z. Qing, Nucl. Data Sheets **68**, 887 (1993).